Can there be an Earth-like planet in HD 37605?

Johan Appelgren

Lund Observatory
Lund University

2017-EXA124

Degree project of 15 higher education credits
May 2017

Supervisor: Melvyn Davies

Lund Observatory
Box 43
SE-221 00 Lund
Sweden

Abstract

Detection of Earth-mass planets on orbits around 1 AU with the radial velocity method has so far not been possible, the Doppler velocity they induce on their host star is too small to be detected. Planetary systems detected with the radial velocity method might then contain undetected Earth-like planets. One such planetary system is HD37605, which contains a star similar to the Sun and two gas giants. One on a highly eccentric low semi-major axis orbit, and one on a near circular orbit almost 4 AU out. In this thesis the possibility that an Earth-like planet, with 1 $M_\oplus$ or 2 $M_\oplus$ masses, can remain on stable orbits within the habitable zone of HD37605 is investigated. This is done by simulating HD37605 with an additional planet for 20 Myr using the Mercury package. Orbits are considered stable if the simulations does not end in an ejection or collision, and they are considered habitable if the additional planet never leaves the habitable zone. It was found that stability varies a lot over the habitable zone. Peak stability occurs at 0.9 AU and 1.2 AU, and peak instability at 1.1 AU. Habitable runs were found in a region between 0.95 AU and 1 AU. This was the only region where the eccentricity oscillations induced on the additional planet can remain small enough that the planet does not leave the habitable zone.

Populärvetenskaplig beskrivning

Planeters omloppsbanor är, trots att det kanske verkar så på en tidsskalan som ett mänskligt liv, inte oförenderliga. I planetsystem med två eller flera planeter så påverkar planeterna på varandras omloppsbanor med deras gravitation. Planeterna växelverkar med varandra och ett utbyte av energi och rörelsemängdsmoment sker. Rörelsemängdsmoment är motsvarigtheten till rörelsemängd för saker i rotation. Detta utbyte ändrar planeternas omloppsbanor och kan, med tiden, leda till att planetsystemet blir ostabilt och planeter kolliderar eller kastas ut ur systemet.

I detta projekt så undersökt planetsystemet HD37605. Det är ett system som består av en Sol-lik stjärna med två gasjättar i omloppsbana runt den. Ena gasjätten har en väldigt excentriskt bana mycket nära stjärnan. Den andra har en nästan cirkulär bana och är ungefär fyra gånger så avlägsen från sin stjärna som Jorden är från Solen. Målet med projektet är att undersöka om detta system skulle kunna inehålla en Jordliknande planet med en omloppsbana lik Jordens utan att bli ostabilt. Detta görs genom att simulera systemet på en dator. Omloppsbanorna undersöks sedan för att se om de befinner sig inom den beboliga zonen. Den beboliga zonen är det område kring en stjärna där flytande vatten kan existera. Planeter inom detta område skulle då potentiellt kunna upprätthålla liv.

Man kan fråga sig vad mening med att simulera att det finns ytterligare en planet i HD37605 är när vi redan observerat systemet och sett att det finns två planeter. Dessa två planeter upptäcktes dock med en metod som inte är känslig nog för att upptäcka en så liten planet som Jorden på en omloppsbana inom den beboliga zonen. Så om en sådan planet skulle finnas där så sulle vi inte upptäcka den med dagens teknologi. Möjligheten finns alltså att det existerar en oupptäckt, potentiellt bebolig, planet i planetsystemet HD37605.

Contents

List of Figures

List of Tables

Chapter 1

Planet interactions

1.1 How planets interact

In systems consisting of multiple planets, the planets will interact through the mutual gravitational pull they exert on each other. As a consequence of this, the orbits of these planets change over time. If these changes cause planets to move within each other's mutual Hill radii (which is defined in section 1.2) they experience a close encounter. These close encounters can in turn cause planetary systems to become unstable. If planets experience multiple close encounters and the strength of the interactions grow this can lead to the ejection of a planet, or if not enough energy is exchanged in these scatterings, the planets can come physically close enough to each other to collide.

Planet-planet interactions are driven by the exchange of energy and angular momentum between the planets (Davies et al. 2014). The semi-major axis and eccentricity of an orbit are determined by the energy and angular momentum, so an exchange of these between two planets will cause the orbits to change. In the case of a simple two-body problem the energy E and eccentricity e of an orbit is given by

$$E = -\frac{GM_1M_2}{2a}, \tag{1.1a}$$

$$e^2 = 1 + \frac{2EJ^2}{G^2M^2\mu^3}. \tag{1.1b}$$

The energy equation is derived in appendix B and the ecentricity is given in Beutler (2005).[1] G is the gravitational constant, M_1 and M_2 are the masses of the two bodies (the star and the planet), and a is the semi-major axis of the planet. J is the angular momentum, M

[1]Note that in Beutler (2005) the eccentricity is given in terms of specific orbital energy and specific relative angular momentum. They are the energy and angular momentum divided by the reduced mass μ.

the total mass of the system, and μ the reduced mass of the two bodies. The important part here is to see that energy E is only determined by semi-major axis a, and that the eccentricity e is determined by E and angular momentum J. When planets scatter they exchange a random amount of energy and angular momentum, causing their orbits to change. A planet that gains energy will move to a larger semi-major axis and a planet that gives up angular momentum will become more eccentric. If a planet gains enough energy it can thus become unbound and be ejected from the system.

In a closed system, energy and angular momentum must be conserved, so a planet can only change its orbit by exchanging energy and/or angular momentum with another body in the system. In the case of a well separated two planet system the planets interact through the exchange of angular momentum but not energy. This leads to oscillations of inclination and eccentricity between the two planets (Davies et al. 2014). In the case where the two planets are not well separated, or if there are more than two planets, close encounters can occur. Such planetary systems are also chaotic in nature, meaning that a small difference in starting parameters can lead to different outcomes. This makes it difficult to attempt to make predictions about the their future.

There are three outcomes for a planet on an unstable orbit, it can either be ejected from the system, or collide with another planet, or experience a near approach with the host star. The near approach will result in either a collision with the star or a tidal dissipation. In close encounters between two planets the most likely outcome, ejection or a planet-planet collision, can be predicted with what is called the Safronov number, denoted by Θ (Davies et al. 2014). It is defined as

$$\Theta^2 = \left(\frac{M_p}{M_\star}\right)\left(\frac{R_p}{a_p}\right)^{-1}. \tag{1.2}$$

$M_\star$ and M_p are the mass of the host star and the planet respectively. R_p is the radius of the planet and a_p its semi-major axis. What this represents physically is a ratio between the planets surface escape speed and its orbital speed. If this ratio is larger than 1, i.e. the surface escape speed is greater than the orbital speed, scattering tend to lead to ejections. If the ratio is smaller than 1 collisions dominate as the most likely outcome (Goldreich et al. 2004).

1.2 Planetary system stability

There are a number of ways to define what a stable planetary system is. The most basic requirement would simply be that no collisions or ejections of planets has occurred. Using this requirement this does not say anything about the future of a system though. Stricter

requirements are needed if one wishes to attempt to make predictions about the future stability of a system.

A system that does not experience any close encounters is said to be Hill stable. For systems consisting of only two planets it is possible to make a prediction of this. For two planets on non-eccentric co-planar orbits Gladman (1993) showed that the system is Hill stable if the separation in mutual Hill radii between them, denoted Δ, is

$$\Delta_{1,2} = \frac{a_2 - a_1}{R_{Hill,m}} \gtrsim 2\sqrt{3}. \tag{1.3}$$

Where a_1 and a_2 are the semi-major axis of planet 1 and 2, and $R_{Hill,m}$, the mutual Hill radii, is defined as

$$R_{Hill,m} = \left(\frac{M_1 + M_2}{3M_\star}\right)^{1/3} \frac{a_1 + a_2}{2}. \tag{1.4}$$

M_1, M_2, a_1, and a_2 are the masses and semi-major axis of the two planets, and $M_\star$ is the mass of the star.

A two planet system can still be stable if $\Delta < 2\sqrt{3}$. Hill stability just gives a limit at which a system is guaranteed to not experience close encounters, not a limit where below it, the system must become unstable. Systems with $\Delta < 2\sqrt{3}$ may still be stable although it is not guaranteed. For systems with more than two planets there is no analytical criteria for a system to be Hill stable. Chambers et al. (1996) investigated the stability of such planetary systems with more than 2 planets. They found that systems with $\Delta < 10$ always become unstable given enough time. The time until the first close encounter can be modeled by

$$\log t = b\Delta + c, \tag{1.5}$$

with b and c being constants depending on the number of planets. For equal mass planets the slope b decreases from 3 to 5 planets, but does not change much for a further increase in the number of planets. (Chambers et al. 1996). From this one sees that the value of Δ sets the time scale for instabilities to occur. In systems with more than 2 planets there will of course be more than one Δ value, it is the minimum of these that sets the timescale. This time scale is in fact an incredibly strong funtion of Δ, increasing the separation between planets in Hill radii by a factor of two can increase the number of orbits required before instability beings by a factor of more than 10^5, see fig. 1 in Davies et al. (2014).

A stricter requirement still is the so called Lagrange stability. For a system to be Lagrange stable both planets must be bound and ordered, meaning the orbits of the planets will not cross and no collisions occur, for all time (Veras & Mustill 2013). However, as with Hill stability for more than two planets, no analytical criteria that gives Lagrange stability is known.

Another factor which can change system stabilities are orbital resonances. These resonances are simply the ratios between the orbital periods of planets. If two planets are in a resonance, say a 2:1 resonance so the one planet completes two orbits for every one orbit the other completes, the planets will be aligned at the same positions in space with a regular frequency. The planets will then pull on the same spot in the orbit regularly. This can clear out certain regions in space. An example of this are the Kirkwood gaps in the asteroid belt. They are region cleared out of asteroids by mean motion resonances with Jupiter (Kirkwood 1866). Resonances can also have a stabilizing effect on systems as well, such as the 4:2:1 resonance of Jupiters moons Ganymede, Europa, and Io (Karttunen et al. 2007).

Chapter 2

HD37605

2.1 HD37605 system

HD37605 is a star with a planetary system located 44 pc away in the Orion Constellation. It consists of two gas giants orbiting a star similar to the Sun. Its planets were detected using the radial velocity method. As a consequence of the limited sensitivity of current spectrographs, it is very difficult or impossible to detect low mass planets with the radial velocity method unless they are orbiting extremely close to their host star. A 1 $M_\oplus$ planet orbiting on a circular orbit with semi-major axis 1 AU around a 1 $M_\odot$ star (like HD37605) would produce a radial velocity signal of about 9 cm s^{-1}. Spectrographs that have been active in the past decade or so, such as HARPS are not able to achieve this level of precision (Pepe et al. 2014). In this project the possibility that such an undetected Earth-like planet could exist and remain stable in the habitable zone around HD37605 is investigated. This additional planet will be referred to as planet *d*.

As it is known to us the star in HD37605 is a of mass 0.98 $M_\odot$, radius 0.89 $R_\odot$, and effective temperature $T_{eff} = 5380$ K (Bonfanti et al. 2015). The planets, named HD37605b, and HD37605c, are both gas giants. HD37605b has a mass of $M_b \sin i = 2.813$ M_{Jup} and sits on a highly eccentric orbit, $e_b = 0.6767$, with semi-major axis $a_b = 0.2837$ AU. HD37605c is somewhat more massive with a mass of $M_c \sin i = 3.366$ M_{Jup}. It has a near circular orbit with $e_c = 0.013$ at a semi-major axis of $a_c = 3.814$ AU (Wang et al. 2012). A figure of the structure of HD37605 with planet d can be seen in fig. 2.1.1.

Due to how well separated the two known planets in HD37605 are, it is not expected that they will display any unstable behaviour on their own. Their mutual Hill radii is $\Delta_{bc} = 13.75$, if their $M \sin i$ masses are assumed to be the actual masses. Altough it is not strictly applicable for noncircular orbits like these planets have, one can compare this to the requirement of $\Delta \gtrsim 2\sqrt{3}$ for circular orbits to be Hill stable. Δ_{bc} is much greater than this, so HD37605 should be a stable system. It is possible that the planets are

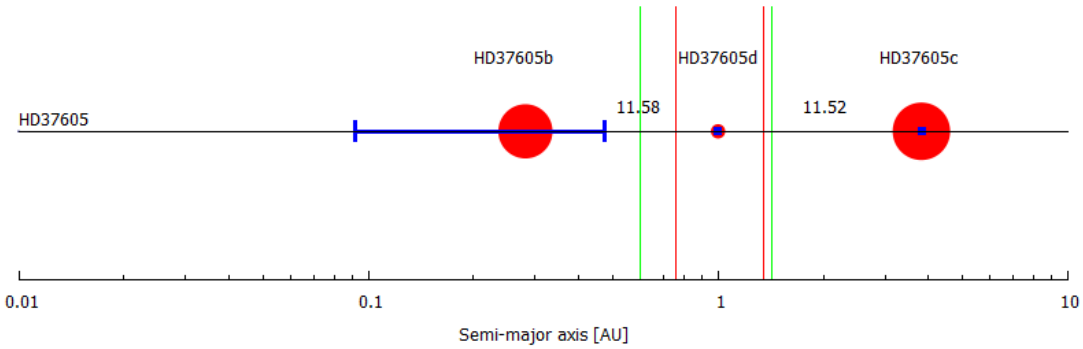

Figure 2.1.1: Structure of HD37605 with the additional planet at 1 AU. The blue region represent the range between periapsis and apoapsis for each planet. The number between the planets are the mutual Hill radii with a 1 $M_\oplus$ additional planet and either of the two known planets, Δ_{bd} and Δ_{dc}. The vertical red and green lines shows the limits of a conservative and optimistic habitable zone respectively. Note: The two gas giants are to scale with each other but the additional smaller planet is not.

quite a lot more massive than the measured $M \sin i$ masses. This is unlikely to make the system unstable though, Wang et al. (2012) performed a 10^8 year coplanar integration with $1/\sin i = 10$, giving the planets masses ~ 30 M_{Jup}. The system displayed no instability and the amplitude of the eccentricity oscillations only doubled.

2.2 The habitable zone around HD37605

As the aim of this project is to investigate the possibility that an additional Earth-like planet can remain on a stable orbit in the habitable zone around HD37605, this requires an estimate of the range of the habitable zone around HD3765. The results of this are shown in table 2.1.

The habitable zone, from here on abbreviated as HZ, is typically defined as the region in space around a star where a planet can maintain liquid water on its surface. Determining the boundaries for the HZ can be a difficult task. The boundaries will depend on several different factors, such as atmosphere and planet mass. Most significant of these factors is the amount of solar flux that arrives at a planet, and as such the luminosity of the star and the planets distance to it. To estimate the HZ in HD37605 a model by Kopparapu et al.

Table 2.1: The conservative and optimistic edges of the HZ for a 1 $M_\oplus$ are shown below. The conservative edges are limited by what is called the moist greenhouse effect for the inner edge and the maximum greenhouse effect for the outer edge. The optimistic outer edge is based on a belief that Mars had liquid water 3.8 Gyr ago. The inner optimistic edge is based on the assessment that Venus has not had liquid water for at least 1 Gyr.

Conservative HZ		Optimistic HZ	
Inner edge [AU]	Outer edge [AU]	Inner edge [AU]	Outer edge [AU]
0.759	1.353	0.599	1.426

(2013b), Kopparapu et al. (2013a) is used. Their work is in turn based on an earlier model made by Kasting et al. (1993). The model they used to estimate the HZ is a one dimensional radiative-convective, cloud free climate model. The planet used in the model is a 1 $M_\oplus$ planet with either an H_2O or CO_2 dominated atmosphere. The H_2O dominated atmosphere is used for the inner edge of the HZ and the CO_2 dominated one is used for the outer edge. The model works by specifying a surface temperature and calculating the required solar flux to sustain this temperature. This is called inverse climate modeling.

Depending on what conditions one uses for the boundaries different estimates of the HZ can be made. Both a conservative and a more optimistic estimate is made, abbreviated the CHZ and OHZ respectively.

The inner limit of the CHZ is based on what is called the moist greenhouse effect as its limit. At this limit the stratosphere of the planet becomes dominated by water. The water is then broken up by photolysis and hydrogen quickly escapes the atmosphere. The outer edge is limited by the maximum greenhouse effect. Planets in this region can develop dense atmospheres rich in CO_2. But, close to the outer edge the CO_2 in the atmosphere condenses, leading to a reduction in the greenhouse effect. Furthermore, CO_2 is a very prominent Rayleigh scatterer, so a CO_2 rich atmosphere will have a high albedo. A high albedo counteracts the greenhouse effect of the CO_2 rich atmosphere, cooling the atmosphere. The outer limit is then taken as the point at which the Rayleigh scattering becomes more prominent than the greenhouse effect.

The optimistic estimates are empirical in nature. The outer edge is based on the belief that Mars had liquid water about 3.8 billion years ago. This is called the early Mars limit. From this one can calculate the solar flux that Mars received at that time and use this as a limit for the necessary flux. The inner edge estimate, called the recent Venus limit, is made from a similar assessment that Venus has not had liquid water for at least 1 billion years.

The habitable zone also moves with changing planet mass. For more massive planets the inner edge will move slightly inwards and slightly outwards for less massive planets. For a 5 $M_\oplus$ planet the inner edge moves inwards about $\sim 7\%$. The outer edge does not change

Table 2.2: Constants used to calculate S_{eff} (Kopparapu et al. 2013a).

	Recent Venus	Moist greenhouse	Maximum greenhouse	Early Mars
$S_{eff,\odot}$	1.7763	1.0146	0.3507	0.3207
a	$1.4335 \cdot 10^{-4}$	$8.1884 \cdot 10^{-5}$	$5.9578 \cdot 10^{-5}$	$5.4471 \cdot 10^{-5}$
b	$3.3954 \cdot 10^{-9}$	$1.9394 \cdot 10^{-9}$	$1.6707 \cdot 10^{-9}$	$1.5275 \cdot 10^{-9}$
c	$-7.6364 \cdot 10^{-12}$	$-4.3618 \cdot 10^{-12}$	$-3.0058 \cdot 10^{-12}$	$-2.1709 \cdot 10^{-12}$
d	$-1.1950 \cdot 10^{-15}$	$-6.8260 \cdot 10^{-16}$	$-5.1925 \cdot 10^{-16}$	$-3.8282 \cdot 10^{-16}$

noticeably however.

The formula used to calculate the HZ edges is

$$d = \frac{L/L_{\odot}}{S_{eff}} \tag{2.1}$$

Where L and $L_{\odot}$ are the luminosity of the star and the Sun respectively. S_{eff} is given by calculating

$$S_{eff} = S_{eff,\odot} + aT_{\star} + bT_{\star}^2 + cT_{\star}^3 + dT_{\star}^4 \tag{2.2}$$

(Kopparapu et al. 2013b). Values of the coefficients $S_{eff,\odot}$, a, b, c, and d are shown in table 2.2. $T_{\star}$ is defined as $T_{\star} = T_{eff} - 5780$ K. The resulting HZ edges are shown in table 2.1.

Chapter 3

Exploring HD37605

As stated, the aim of this project is to look for the possibility that an Earth-like planet could exist on stable orbits in the habitable zone in HD37605. It is not an attempt to look for such a planet, but merely an attempt to look for stable orbits given that the system is structured as described. To achieve this HD37605 was simulated using the Mercury N-body integrator.

3.1 Mercury, a short description

Mercury is a hybrid symplectic integrator originally written by Chambers (1999). The biggest advantages of symplectic integrators is that they have no long term build up of energy error (which is important since energy must be conserved in a closed system), other than what is caused by computer round off, and that they are very fast. The main disadvantage when integrating planetary systems is that they become inaccurate whenever dealing with two planets that are close to each other.

Symplectic integrators work by splitting the Hamiltonian in parts which can each be solved on its own. It is split into a dominant part and a small perturbation part. For a planetary system the dominant part is the gravitational force from the star, and the small perturbation is the interaction between planets or other smaller bodies in the system. The problem that arises when two planet are close to each other is that their interaction no longer is a small perturbation, which causes large errors in the integration. To solve this problem Mercury moves the previously weak interaction of two planets from the small perturbation part to the dominant part when there is a close encounter of said planets. Practically, this is achieved by letting the equation for the planet-planet interaction be part of both the dominant and small perturbation part at all times. A factor is then included which is dependant on the separation between two planets. This factor makes it so that when two planets are close to each other, the calculation of these two planets interaction van-

ishes in the perturbation part. Similarly when two planets are not close to each other the calculation of their interaction vanished in the dominant part.

3.2 Initial conditions

The known parameters of the planets in HD37605 are shown in table 3.1. The planets were also given the same densities as Jupiter, $\rho = 1.33$ g/cm^3 (Williams 2016), since they are both of similar mass to Jupiter. It is also assumed that the planet orbits were observed edge on when detected, so the $M \sin i$ masses are the actual masses.

Table 3.1: The known physical and orbital parameters of the planets in HD37605 are listed below (Wang et al. 2012).

Planet	Mass ($M \sin i$) [M_{Jup}]	a [AU]	e	ω [°]
HD37605b	2.813 ± 0.032	0.2837 ± 0.0016	0.6767 ± 0.0019	220.86 ± 0.27
HD37605c	3.366 ± 0.072	3.814 ± 0.058	0.013 ± 0.015	221 ± 78

Since the planet that was added to the system was supposed to be Earth-like it was given some of the same characteristics as Earth, namely the same eccentricity, $e = 0.0167$ (Simon et al. 1994) and density $\rho = 5.51$ g/cm^3 (Williams 2016). The unknown orbital parameters of all three planets were randomly generated according to the method given by Johansen et al. (2012). Inclinations were generated randomly from a uniform distribution between 0° and a inclination parameter β. β was given a value of $\beta = 3°$, giving the orbits mutual inclinations between 0° and 6°. In the same way, mean anomaly, argument of periapsis and longitude of ascending node (for the additional planet only) were randomly generated from a uniform distribution between 0° and 360°. The energy of the system needs to be conserved throughout a simulation, however, there will a change in energy due to computational restrictions, such as round of errors. The size of the energy change will depend in part on the time step used in the simulation. A time step of 1 day is used as with this step size only very few runs had a fractional energy change $\frac{\Delta E}{E} > 10^{-3}$, with the majority having a change in the region of $\frac{\Delta E}{E} \approx 10^{-5}$. $\frac{\Delta E}{E} < 10^{-3}$ was chosen as an appropriate energy limit following Mustill et al. (2015).

At first a set of 25 runs were made without adding an additional planet. This was done to confirm that the system is stable as is and does not display any behaviour indicating that it might become unstable within the time scale of the simulations. Each run lasted 20 Myr.

Initial runs of HD37605 with the additional planet were made with a 1 $M_\oplus$ additional planet at semi-major axis positions of 0.8 AU, 1 AU, and 1.2 AU. A total of 48 were made for each semi-major axis position with each run lasting 20 Myr. After these runs were

Table 3.2: Separations between planets in mutual Hill radii. The difference between the two masses of planet d is very small. This is not surprising since the mass of the planets b and c are the dominant ones.

	$M_d = 1\ M_\oplus$							$M_d = 2\ M_\oplus$		
Semi-major axis	0.8	0.9	0.95	1	1.05	1.1	1.2	0.8	1	1.2
Δ_{bd}	9.884	10.80	11.20	11.58	11.92	12.24	12.81	9.880	11.57	12.81
Δ_{dc}	12.77	12.08	11.75	11.42	11.11	10.79	10.19	12.76	11.42	10.19

finished the same process was repeated but for a 2 $M_\oplus$ planet, with the same number of runs.

Once both masses of the additional planet had been simulated at 0.8 AU, 1 AU and 1.2 AU the 1 $M_\oplus$ planet was looked into in more detail. Another set of 48 runs at 0.9 AU and 1.1 AU, and then another 32 runs at 0.95 AU and 1.05 AU were made in order to further refine the result.

3.3 Requirements for stability and habitability

3.3.1 Stability

In this project stability is determined by seeing if a planet has been ejected from the system, or if there have been any collisions between planets or between the star and a planet.

By calculating the Δ values at the different semi-major axes the additional planet was placed at one can try to predict which orbits should be the most stable. The result of this can be seen in table 3.2. The minimum at each semi-major axis is plotted in figure 3.3.1. Since the lowest value of Δ at each semi-major axis set the time scale for instability one would from this plot expect stability to peak at 1 AU, since it has the highest minimum Δ, and drop of towards 0.8 AU and 1.2 AU.

3.3.2 Habitability

The requirement for an orbit of planet d to be classified as habitable is that the planet does not leave the HZ at any point during the simulation. The range of separations from the star that a planet covers is given by the minimum distance to the start r_{min}, called periapsis,

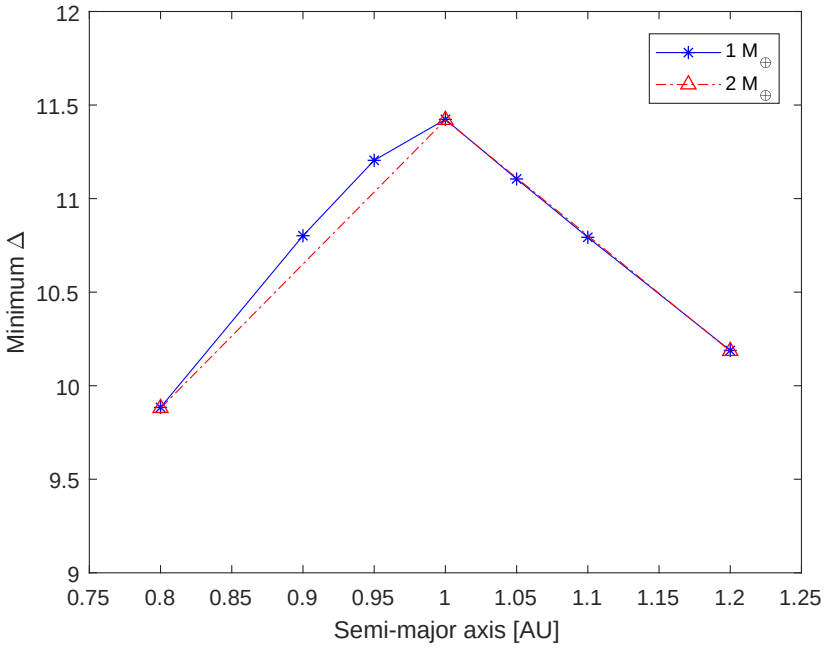

Figure 3.3.1: Minimum Δ value at the initial semi-major axes tested. The minimum Δ values sets the time scale for instability to occur. This is because the value of Δ is inversely proportional to the strength of planet interactions, and stronger interactions causes earlier instability. From this one would expect stability to be highest at 1 AU since it has the highest minimum Δ.

and the maximum distance r_{max}, called apoapsis. These are calculated from

$$r_{min} = (1 - e)a \tag{3.1a}$$
$$r_{max} = (1 + e)a. \tag{3.1b}$$

Using the edges of the HZ given in table 2.1 and setting them as r_{min} and r_{max} one can calculate the maximum eccentricities allowed for a planet to remain within the HZ at the initial semi-major axes used. The results of this can be seen in table 3.3. This will not be the exact limit as there are small oscillations in semi-major axis in time, which will be slightly different for each run due to the chaotic nature of planetary systems. This means these values will be somewhat over estimated since the oscillations in semi-major axis will move the planet closer to the edge of the HZ. If at a time where the semi-major axis is closer to the edge, the eccentricity is also high, the planet will move out of the HZ with a lower eccentricity than the maximum values calculated here. In the same way however, a point of low semi-major axis might have slightly higher eccentricity tolerance. That will depend of whether the semi-major axis is closest to the outer or the inner edge of the HZ. However, since the amplitude of the oscillations are not known beforehand, and each run oscillates differently, these estimates of the maximum allowed eccentricity do not take this into account.

Table 3.3: The maximum eccentricity that is allowed for a planet that remains on its initial semi-major axis to remain within the optimistic habitable zone and the conservative habitable zone.

Semi-major axis [AU]	0.8	0.9	0.95	1.0	1.05	1.1	1.2
Conservative ecc. limit	0.060	0.164	0.208	0.248	0.278	0.220	0.1183
Optimistic ecc. limit	0.256	0.340	0.375	0.406	0.347	0.286	0.1783

As far as determining if a run leaves planet d within HZ, the periastron and apastron are calculated using the eccentricity and semi-major axis of each data point. So overestimating the maximum allowed eccentricity here does not affect the determination of which runs are habitable or not.

Carrera et al. (2016) set a limit for habitability that the mean irradiation reaching the planet does not change by more than 10%. For an orbit with initial eccentricity of 0.0167, as used here, this corresponds to a maximum eccentricity of 0.4169. This was also intended to be used in this project, but since this eccentricity limit is higher than the limits from table 3.3 it proved superfluous. Planet d will leave the HZ before it reaches an eccentricity of 0.4169 for all initial semi-major axes that were used.

Chapter 4

Results

4.1 HD37605 without an additional planet

The planets in HD37605 as it is known remain stable showing no sign of any changes in eccentricity and semi-major axis other than what is caused by the oscillations between them, which has period of $P = 5.11 \cdot 10^5$ yr $\pm$ $2.20 \cdot 10^4$ yr. This result is unsurprising given the large separation between the two planets. A plot of the eccentricity oscillations of the two planets can be seen in fig. 4.1.1. The planets oscillate with a regular period without any indication that they might become unstable within the 20 Myr time frame of the simulations.

4.2 HD37605 with an additional planet

4.2.1 Stability

The fraction of runs that become unstable at each semi-major axes that was looked at can be seen in fig. 4.2.2. All runs are stable at 0.9 AU and 1.2 AU, and at all other tested semi-major axes some runs become unstable, with peak instability at 1.1 AU. This result is surprising since from the prediction made in section 3.3.1, using the minimum Δ value at each semi-major axis, which can be seen in fig. 3.3.1, one would expect peak stability at 1 AU since it has the highest minimum Δ. Stability is expected to decrease with increasing and decreasing semi-major axis. Going out to 0.95 AU and 1.05 AU follows this behaviour, both being having more unstable runs than 1 AU. Outside of this, the instability behaves surprisingly, at 0.9 AU more runs should become unstable than at 0.95, but instead no runs became unstable there. Similarly, more runs should become unstable at 1.2 AU than at 1.1 AU, but also at 1.2 AU stability increases unexpectedly. There appears to be some other effect at work that causes distribution of instability.

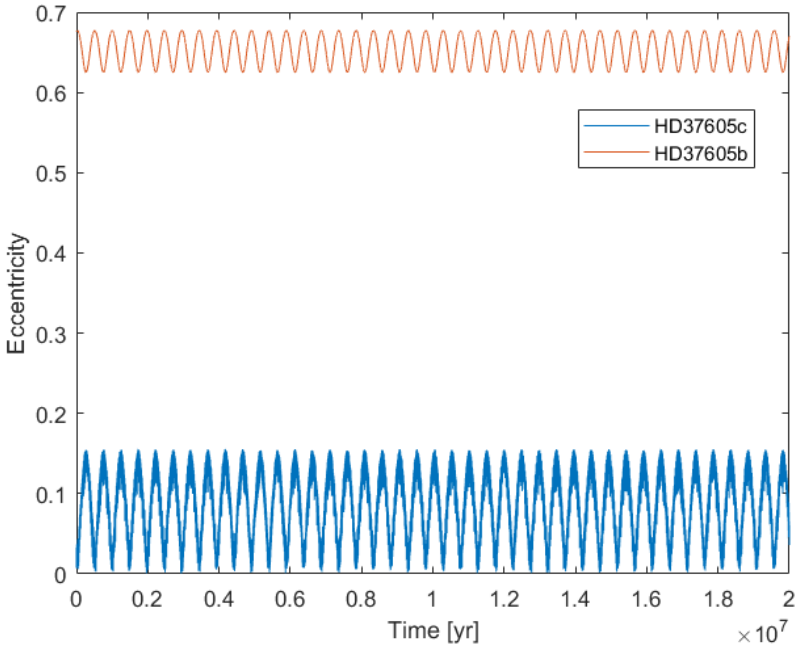

Figure 4.1.1: Eccentricity oscillations of HD37605 over 20 Myr. Both planets oscillate steadily with a period of $\sim 5 \cdot 10^5$ yr. No signs of potential instability can be seen.

Fig. 4.2.1 show cumulative distribution of unstable runs over time. None of the plots appear to shown any significant structure, at all semi-major axes instability seems to increase steadily with time. It does appear as if the 2 $M_\oplus$ planet becomes unstable at slightly later times than then 1 $M_\oplus$ planet. This is unexpected since a 2 $M_\oplus$ planet will have stronger interactions with the other planets, and should if anything become unstable faster. However, this effect may be entirely due to the large errors caused by the small number of runs that do become unstable. At 1 AU there are 4 unstable runs with 1 $M_\oplus$, and 3 unstable runs with 2 $M_\oplus$. Since the error will go roughly as the square root of the number of unstable runs, the error here are taken as $\frac{\sqrt{N}}{N}$, where N is the number of unstable runs. The error with 1 $M_\oplus$ is $\pm$ 50%, and $\pm$ 58% with 2 $M_\oplus$. Similarly at 0.8 AU there are 11 and 10 unstable runs with 1 $M_\oplus$ and 2 $M_\oplus$ respectively. This gives the errors $\pm$ 30% with 1 $M_\oplus$ and $\pm$ 32% with 2 $M_\oplus$. Given these large errors, the difference between 1 $M_\oplus$, and 2 $M_\oplus$ can safely be neglected. A consequence of estimating the errors this way is that the error at 0.9 AU and 1.2 AU is 0%. There is of course some degree of error at these points as well, but it remains unknown with this method.

A more detailed look at the outcome for planet *d*, ejection or a collision with either the star or a planet, can be seen in table 4.1, and 4.2. Here there are also small differences between the 1 $M_\oplus$, and 2 $M_\oplus$ planet. Using the same argument as for the difference between the fraction of runs that become unstable with a 1 $M_\oplus$ and a 2 $M_\oplus$, the difference in outcomes between 1 $M_\oplus$ and 2 $M_\oplus$ can also be neglected.

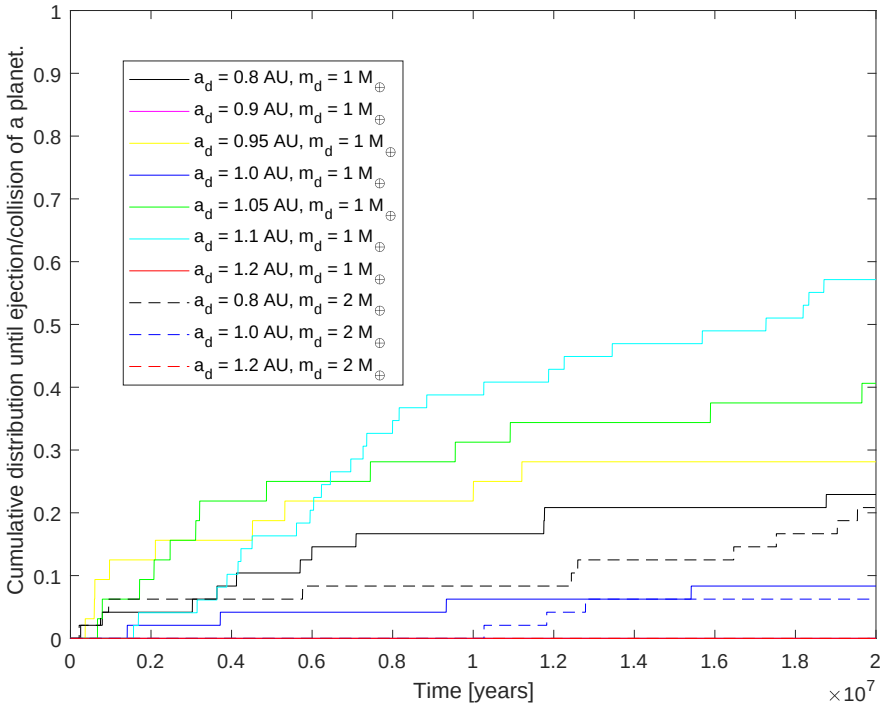

Figure 4.2.1: The cumulative distribution until collision or ejection of a planet. The solid plots are with an additional planet of mass 1 $M_\oplus$ and the dashed plots are a 2 $M_\oplus$ planet.

A possible cause of the unexpected stability distribution over the initial semi-major axes could be mean motion resonances between the planets. Resonances can both serve to stabilize and destabilize orbits, possibly providing an explanation for the observed stabilities. Making a simple comparison between the periods of planet b and c with the periods of planet d at the different semi-major axes show no clear resonances however. Some positions are near resonances, with planet b and planet d at 0.95 AU being close to a 6:1 ratio, and a 7:1 ratio when planet d is at 1.05 AU. Both 0.95 AU and 1.05 AU are semi-major axes where the stability behaves similarly to how one would expect from the Δ values though. Based on that is seems unlikely that these resonances would cause instabilities. Potential resonances at the different semi-major axes examined should be looked into more deeply.

As briefly discussed in section 1.1 planetary systems are very chaotic, that is a small change in initial conditions can lead to vastly different outcomes. To illustrate this, one of the runs with the 1 $M_\oplus$ planet at 1 AU were repeated but with the true anomaly, which is the position of the planet on its orbit measured in degrees from the argument of periapsis, of planet d shifted by 10° in either direction. The orbits were all the same, but with the starting position of planet d shifted slightly. The resulting eccentricity oscillations of all three runs can be seen in fig. 4.2.3. After only 50 000 years there is a noticeable divergence

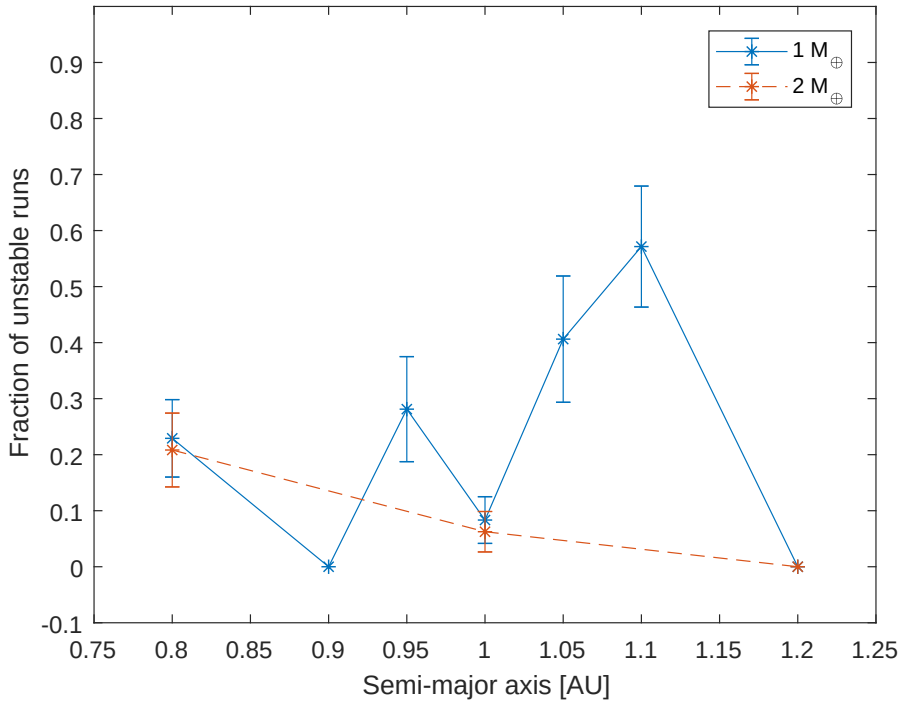

Figure 4.2.2: The fraction of runs that become unstable as a function of semi-major axis. The stability does not follow what one could predict from the minimum Δ values, which would predict peak stability at 1 AU and decreasing stability on either side of this.

between the three runs.

4.2.2 Habitability

Habitable orbits were found in a small region of initial semi-major axis between 0.95 AU and 1 AU for the 1 $M_\oplus$ planet. Habitability among stable runs is highest at 0.95 AU, with 57% habitable runs out of 23 stable runs. At 1 AU the habitability is lower with 36% out of 44 stable runs. For the 2 $M_\oplus$ planet habitable orbits were found at 1 AU with 38% habitable runs out of 45 stable runs. The difference between the two masses is negligible considering the number simulations that were made. The fraction of habitable stable runs plotted over semi-major axis can be seen in figure 4.2.4. Setting 0.95 AU as the initial semi-major axis was not looked at for the 2 $M_\oplus$ planet, but habitable orbits probably exist at 0.95 AU here as well. Looking at the distribution of eccentricities in fig. 4.2.5, one can see that the difference between the different planet masses are negligible at 0.8 AU, 1 AU, and 1.2 AU. There is no reason to believe that it would be any different at other semi-major axes. Habitability limits should then be similar, since for a given semi-major axis eccentricity sets the distances for periapsis and apoapsis according to eq. 3.1a and

Table 4.1: The final outcome of planet d when it had a mass of 1 $M_\oplus$ additional planet. 48 runs were made at 0.8 AU, 0.9 AU, 1 AU, 1.1 AU, and 1.2 AU. At 0.95 AU, and 1.05 AU only 32 runs were made. One should keep in mind that this causes the errors at 0.95 AU and 1.05 AU to be larger.

Initial semi-major axis of planet d [AU]	Survival	Ejection	Planet-star collision	Planet-planet collision
0.8	77%	19%	4%	0%
0.9	100%	0%	0%	0%
0.95	72%	22%	3%	3%
1.0	92%	8%	0%	0%
1.05	59%	31%	9%	0%
1.1	44%	51%	5%	0%
1.2	100%	0%	0%	0%

Table 4.2: The final outcome of planet d when it had a mass of 2 $M_\oplus$ additional planet. 48 runs were made at each semi-major axis.

Initial semi-major axis of planet d [AU]	Survival	Ejection	Planet-star collision	Planet-planet collision
0.8	79%	13%	8%	0%
1.0	94%	6%	0%	0%
1.2	100%	0%	0%	0%

3.1b. The inner edge of the HZ should also move inwards slightly for the 2 $M_\odot$ planet, improving the habitability rate. Such an effect was not taken into account in this analysis. In light of this the fraction of habitable runs is probably slightly underestimated for the 2 $M_\oplus$ planet.

The ranges covered by stable runs of the 1 $M_\oplus$ planet at initial semi-major axis 1 AU can be seen in fig. 4.2.6. Similar plots for the other combinations of mass and semi-major axis can be found in appendix A. The horizontal lines show the range covered by the runs and the vertical lines are the limits of the optimistic (green) and the conservative (red) habitable zones. The colours of the different runs do not mean anything, they are merely there as a visual aid. From the 0.95 AU plot one can see that it is the inner edge of the optimistic HZ which is the side that makes runs leave the HZ. All runs are near the inner edge of the optimistic HZ, with a large fraction of them staying inside it. At 0.9 AU however, all runs have moved outside the inner edge of the optimistic HZ. The same behaviour can be seen when comparing the 1 AU runs with the 1.05 AU runs. Here it is the outer edge of the optimistic HZ at which runs leave the HZ.

To understand why the runs at 0.95 AU and 1 AU remain within the optimistic HZ the

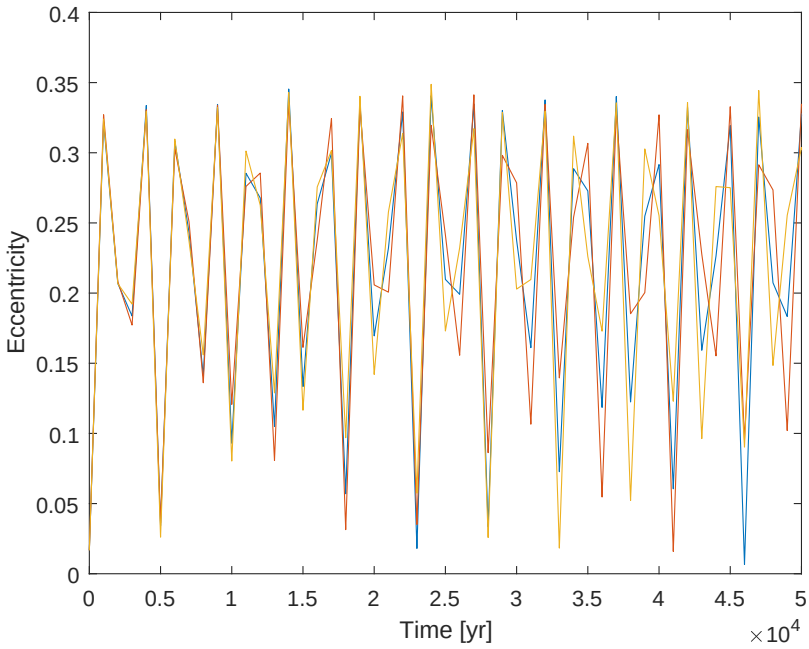

Figure 4.2.3: Three runs with identical orbits but with a mean anomaly difference of 10°. This displays the chaotic behaviour of the system as already after 50 000 yr the eccentricities have diverged noticeably.

median eccentricities can be compared with the maximum eccentricity permitted at that initial semi-major axis. If a run at some points exceeds this eccentricity it is likely to leave the HZ, depending on the semi-major axis at that point in time. Fig. 4.2.7 shows the median, as well as mean eccentricity, and the upper and lower quartile of stable runs at each tested initial semi-major axis for the 1 $M_\oplus$ planet. The upper and lower quartile are the values that 25% of values are higher or lower than respectively. Only at 0.95 AU and 1 AU does the median eccentricity stay below the maximum allowed for the optimistic HZ. The fact that habitability is higher at 0.95 AU can also be understood from this plot. The interquartile range ,the region between the upper and the lower quartile, at 0.95 AU is much smaller than at 1 AU. At 0.95 AU the interquartile range is 0.0193, while at 1 AU it is 0.0675. More telling is that the upper quartile is 0.3857 at 0.95 AU, and 0.4253 at 1 AU. So more stable runs at 1 AU than at 0.95 AU reach the higher eccentricities needed to leave the HZ, causing habitable orbits to be less frequent. Instability is higher at 0.95 AU though. If instead of looking at the fraction of habitable stable runs one looks at the number of habitable runs as a fraction of the total number of runs this brings the fraction of habitable orbits at 0.95 AU and 1 AU closer. Habitability at 0.95 AU is still higher though, with this method 41% out of the 32 total runs are habitable at 0.95 AU and 33% out of the 48 total runs at 1 AU. If the fraction of habitable runs are taken as the fraction of stable runs it is 57% habitable out of 23 stable runs at 0.95 AU and 36% out of 44 stable run at 1 AU. It should be noted also that since fewer runs were made at 0.95 AU than 1

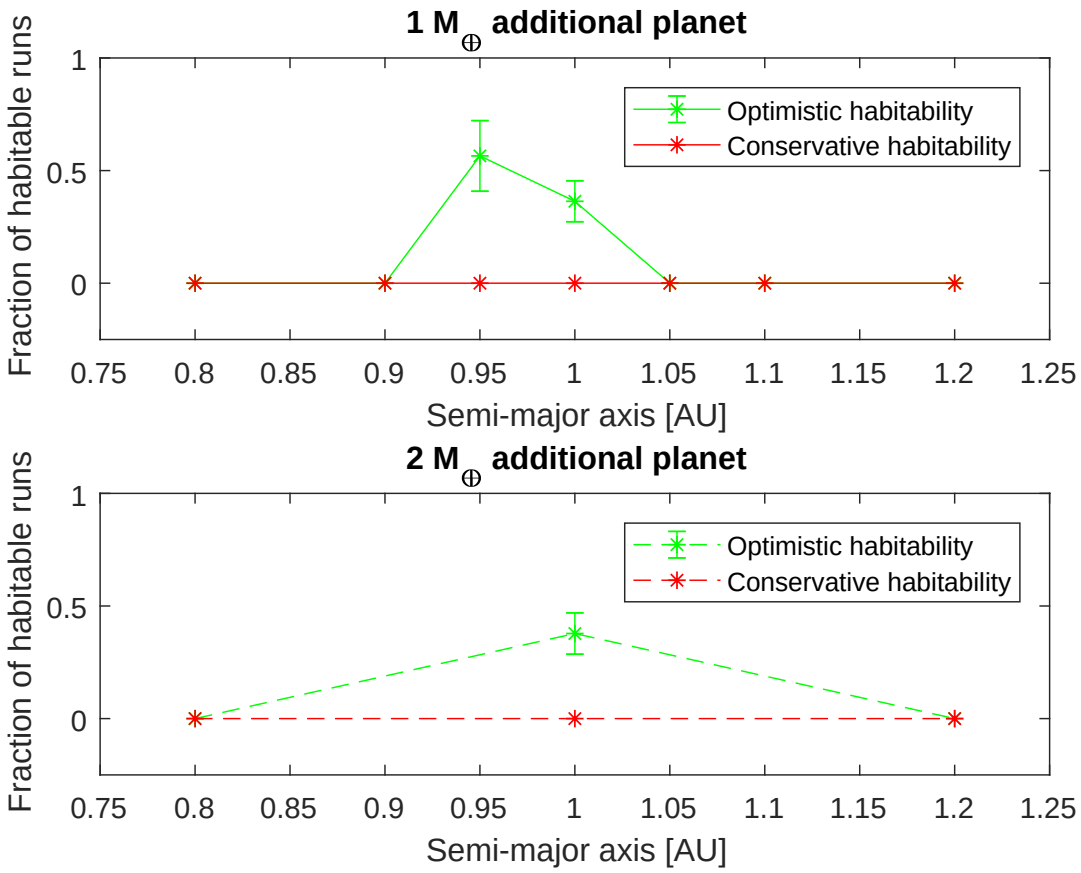

Figure 4.2.4: The fraction of habitable stable runs for both the 1 $M_\oplus$ and 2 $M_\oplus$ planet. The difference in habitability at 1 AU is insignificant considering the limited number of runs.

AU the errors will be larger, as the errorbars in fig. 4.2.4 show.

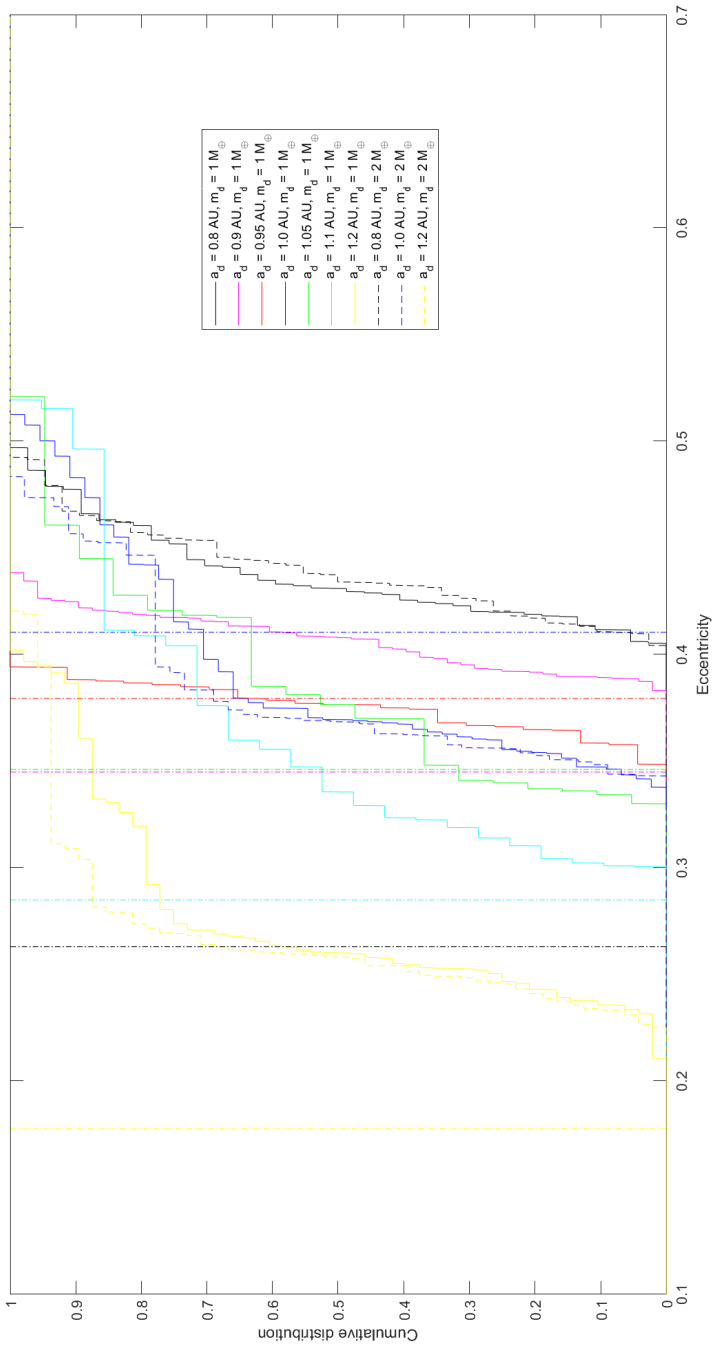

Figure 4.2.5: The cumulative distribution of the maximum eccentricity of planet d from the runs that had not experienced any collisions or ejections by the end of the simulation. The dashed-dotted line show the maximum eccentricity permitted for a planet to remain within the optimistic habitable zone, at its initial semi-major axis. Solid lines are 1 $M_\oplus$ planets and the dashed are 2 $M_\oplus$ planets.

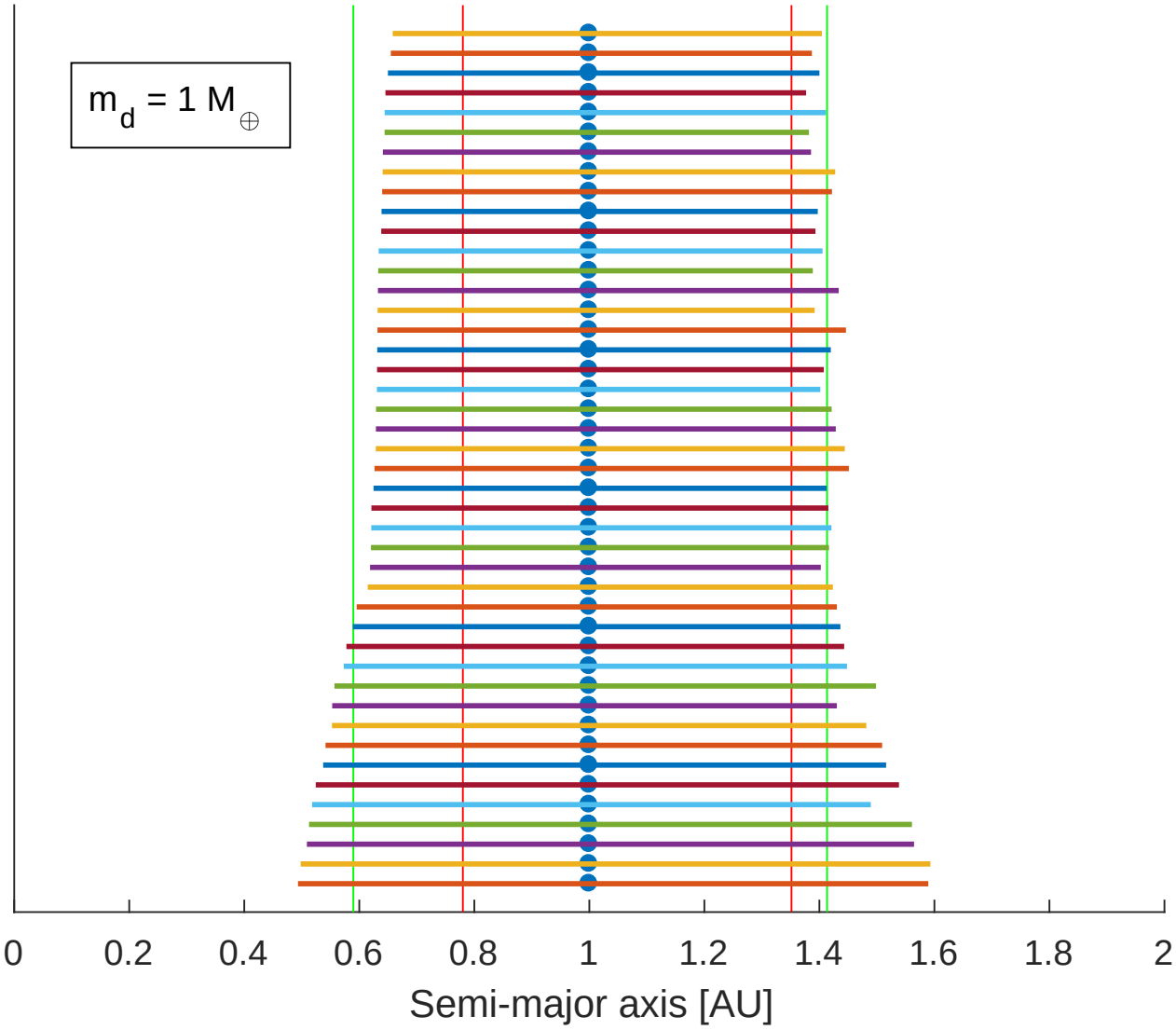

Figure 4.2.6: The range covered by planet d in the stable runs of a 1 $M_\oplus$ planet initially at 1 AU. The vertical red and green lines show the limits of the conservative and optimistic habitable zone respectively. The colours of the different runs are only for visual aid. Similar figures for all combinations of mass and semi-major axis that were tested can be found appendix A.

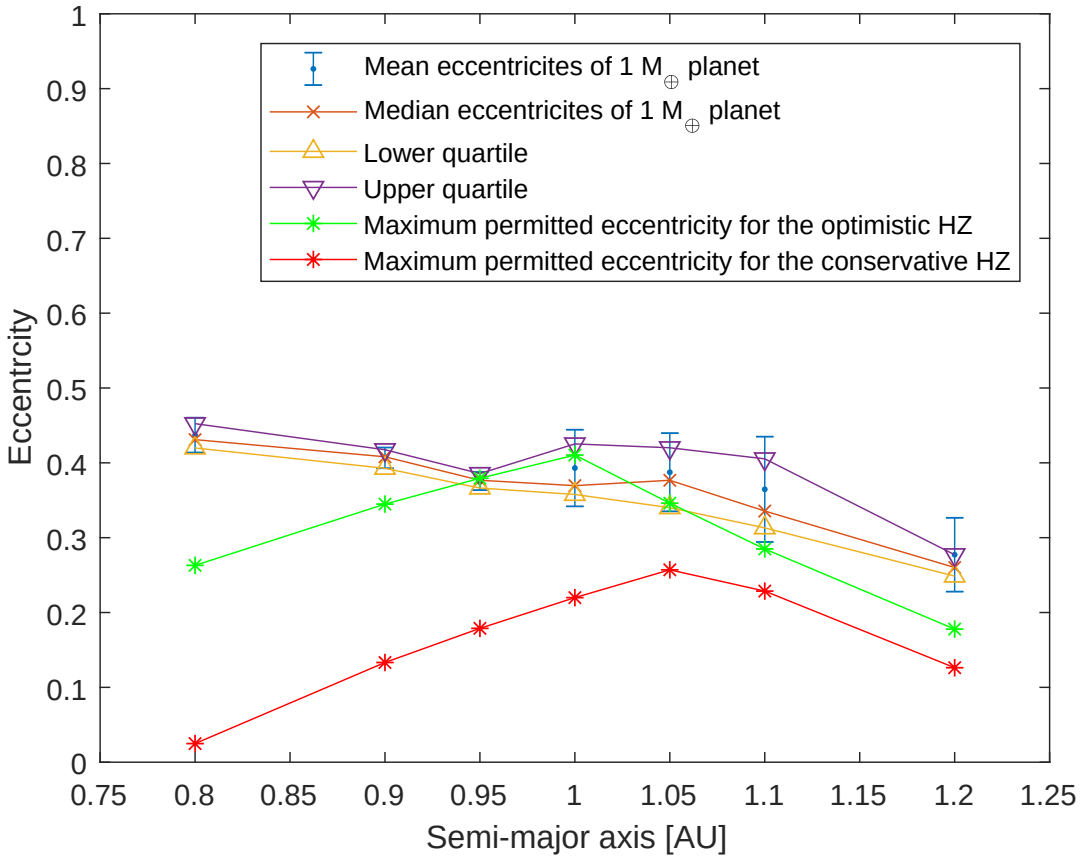

Figure 4.2.7: The mean eccentricities of a 1 $M_\oplus$ additional planet at the tested semi-major axes and the maximum permitted eccentricities before the planet moves outside the HZ. As can be seen none of the positions give a median eccentricity low enough for the planet to remain within the conservative HZ and only at an initial semi-major axis of 0.95 AU and 1 AU is it low enough to remain within the optimistic HZ.

Chapter 5

Conclusions

In conclusion, habitable orbits were looked for in HD37605 and some were found in a small region between 0.95 AU and 1 AU. This is because this is the only region where the eccentricity oscillations induced to planet d are sometimes small enough that the planet remains within the HZ. Having an initial semi-major axis of 0.95 AU seems to be the best spot for habitability since the stable runs at this position have a more narrow distribution of eccentricities, meaning their range of separation from the star is narrower. Stability was lower at initial semi-major axis of 0.95 AU than 1 AU, but even when taking this into account habitable orbits are more likely at 0.95 AU. The fraction of habitable orbits is similar between the two different masses looked at 1 $M_\oplus$ and 2 $M_\oplus$ planet. This is unsurprising since the dominant masses in the interactions are planet b and c. Increasing the mass of planet d by 1 $M_\odot$ only increases the total mass by about one thousand. The strength of the planet interaction should then be similar, an yield similar results.

Stability varies significantly across the range of initial semi-major axis that was examined. The cause of this is not yet fully understood as it seems to contradict what one would expect from the minimum Δ values. A possible reason can be resonances between the planets orbits. But this needs to be further investigated to determine if this is the case or not, as there was not enough time to do a thorough study of this.

5.1 Further research

The limits on habitability in terms of initial semi-major axis can be further refined. As it is now, the outer limit is known to be somewhere between 1.00 AU and 1.05 AU, and the inner limit somewhere between 0.90 AU and 0.95 AU. This can be improved to a more narrow gap. Looking at the figures in appendix A one can see that at 1 $M_\oplus$ and 0.95 AU most runs are very close to the inner edge of the optimistic HZ. This would suggest that the actual lower semi-major axis limit for habitability can not be much lower than 0.95

AU since there is very little margin available. From the 1 $M_\oplus$, 1.05 AU plot some runs are very close to being within the optimistic HZ. The closest one extends about 0.02 AU outside the optimistic HZ, so the upper limit for optimistic habitability is probably around an initial semi-major axis of 1.03 AU.

Stability should increase/decreases with increasing/decreasing planet mass. Exploring how stability would be affected by other masses of planet d would allow one to find a mass limit at which no stable orbits can be found. By calculating the Δ values for a number of different planet masses one can get an estimate for this. Doing this for 0.001 $M_\oplus$, 0.1 $M_\oplus$, 3 $M_\oplus$, 10 $M_\oplus$, 100 $M_\oplus$, and 1000 $M_\oplus$ and plotting the minimum Δ gives the result shown in fig. 5.1.1. At 1000 $M_\oplus$ all minimum Δ values are below 10, which as Chambers et al. (1996) showed, means the system will inevitably become unstable. At 100 $M_\oplus$, Δ is greater than 10 between at least at 0.9 AU to 1.1 AU as initial semi-major axis. So the limit of stability probably lies somewhere between 100 $M_\oplus$ and 1000 $M_\oplus$. However, a 100 $M_\oplus$ planet would have induced a Doppler velocity of 9 m s^{-1} on the star which would put it well within the limit of what is detectable for current spectrographs, such as HARPS that can detect down to 1 m s^{-1} (Pepe et al. 2014). Similarly one could examine the effect of increasing the mass of the other two planets. Since only the $M \sin i$ masses are known it is possible that they have masses quite a lot higher. With this one can determine if there is a point at which planet b and c become to massive for the 1 $M_\oplus$ planet to remain stable.

A deeper study into what causes the instabilities to vary so unexpectedly across the initial semi-major axis range can also be made. The attempt at finding resonances here was only very brief. There might be resonances that were simply not found due the limited search for them.

Something that was not looked into which should be done is the Hill stability with the additional planet. It is possible that some of the runs that were classified as stable have experienced close encounters and are on their way to ejection or collision, but have not yet reached this point. The time scale from first close encounter to ejection/collision was looked into for some of the unstable runs. The longest time that was found was about 70 000 years, with most being between a few thousand and a few tens of thousands. Given this and the 20 Myr length of the simulations it seems likely that most runs that have experienced a close encounter also have had an ejection/collision. With the maximum found time from first close encounter to ejection/collision being 70 000 years, a planet would have to experience its first close encounter sometime within the last 70 000 years of the simulation to have a close encounter but no ejection or collision. With the total time being 20 Myr this is a fairly small window of time. However, all runs have to be looked at to determine whether or not this is the case.

The large eccentricities of planet d's orbit does not necessarily mean it becomes uninhabitable. Given that an ocean is present on a planet its moderating effect on the climate means that it is the time averaged solar flux that is most important of habitability (Williams & Pollard 2002). They give the time averaged flux for an eccentric orbit as

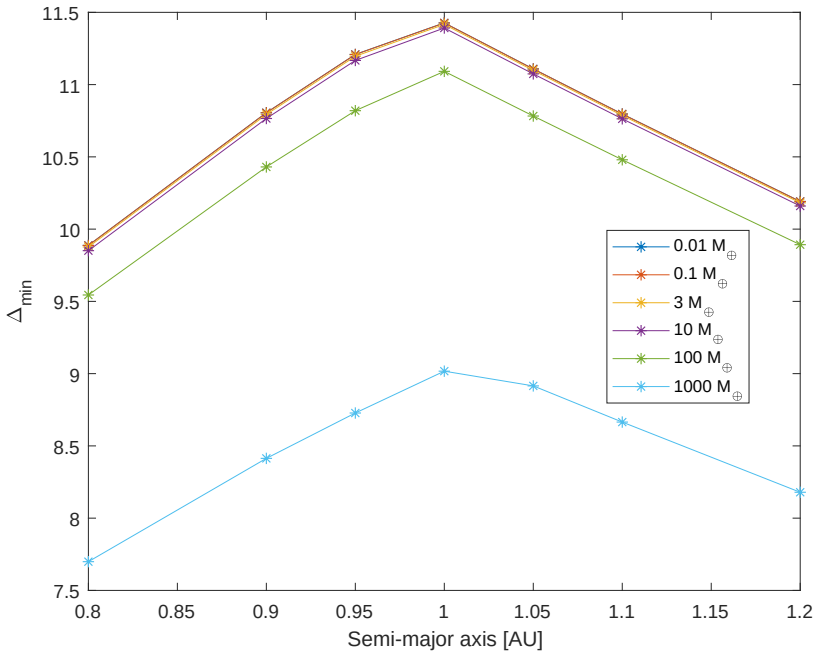

Figure 5.1.1: Minimum Δ values in HD37605 if planet d has masses 0.01 $M_\odot$, 0.1 $M_\odot$, 3 $M_\odot$, 10 $M_\odot$, 100 $M_\odot$, and 1000 $M_\odot$. The minimum Δ value sets the time scale for instability in a system since it is inversely proportional to the strongest interaction in the system.

$$F = \frac{L}{4\pi a^2 (1 - e^2)^{(1/2)}}. \tag{5.1}$$

This shows that the average flux increases with increasing eccentricity. For a planet on a semi-major axis near the outer limit of the HZ a high eccentric might then be beneficial for habitability, since the lowered flux caused by the higher semi-major axis will be compensated by a higher eccentricity. Dressing et al. (2010) showed that a planet with eccentricity 0.5 can be partially habitable out to 1.90 AU, giving more support to the belief that high eccentricities might not be as detrimental to habitability as assumed in this project.

Also worth noting is that a new spectrograph, named ESPRESSO, at the VLT which began operations this year is expected to reach precisions of 10 cm s^{-1}, which would put it within the range of Earth-like planets with semi-major axis at around 1 AU (Pepe et al. 2014). If there is an additional Earth-like planet in HD37605 it might be possible to detect it with this instrument.

Acknowledgements

I would like to thank my supervisor Melvyn for his help with my thesis. He provided me with helpful advice and support, as well as providing motivation and pushing me to do my best. I would also like to thank my friends that I studied with this past semester for any help they provided.

Bibliography

Beutler, G. 2005, Methods of Celestial Mechanics (Springer), 127

Bonfanti, A., Ortolani, S., Piotto, G., & Nascimbeni, V. 2015, A&A, 575, A18

Carrera, D., Davies, M. B., & Johansen, A. 2016, MNRAS, 463, 3226

Chambers, J. E. 1999, MNRAS, 304, 793

Chambers, J. E., Wetherill, G. W., & Boss, A. P. 1996, Icarus, 119, 261

Davies, M. B., Adams, F. C., Armitage, P., et al. 2014, Protostars and Planets VI, 787

Dressing, C. D., Spiegel, D. S., Scharf, C. A., Menou, K., & Raymond, S. N. 2010, ApJ, 721, 1295

Gladman, B. 1993, Icarus, 106, 247

Goldreich, P., Lithwick, Y., & Sari, R. 2004, ApJ, 614, 497

Johansen, A., Davies, M. B., Church, R. P., & Holmelin, V. 2012, ApJ, 758, 39

Karttunen, H., Kröger, P., Oja, H., Poutanen, M., & Donner, K. K. 2007, Fundamental astronomy, 5th edn. (Springer), 176

Kasting, J. F., Whitmire, D. P., & Reynolds, R. T. 1993, Icarus, 101, 108

Kirkwood, D. 1866, Proceedings of American Association for the Advancement of Science for 1866, 8

Kopparapu, R. K., Ramirez, R., Kasting, J. F., et al. 2013a, ApJ, 770, 82

Kopparapu, R. K., Ramirez, R., Kasting, J. F., et al. 2013b, ApJ, 765, 131

Mustill, A. J., Davies, M. B., & Johansen, A. 2015, ApJ, 808, 14

Pepe, F., Molaro, P., Cristiani, S., et al. 2014, Astronomische Nachrichten, 335, 8

Simon, J. L., Bretagnon, P., Chapront, J., et al. 1994, A&A, 282, 663

Szebehely, V. G. & Mark, H. 1998, Adventures in celestial mechanics, 2nd edn. (J. Wiley), 61

Veras, D. & Mustill, A. J. 2013, MNRAS, 434, L11

Wang, Sharon, X., Wright, J. T., Cochran, W., et al. 2012, ApJ, 761, 46

Williams, D. M. & Pollard, D. 2002, International Journal of Astrobiology, 1, 61

Williams, D. R. 2016, Jupiter fact sheet, `https://nssdc.gsfc.nasa.gov/planetary/factsheet/jupiterfact.html` [Accessed: 2017-03-19]

Appendix A

Range covered by orbits of planets on stable orbits

Here are figures of the range covered by planet d all runs for the tested masses and semi-major axes. The vertical red and green lines are the limits of the conservative and optimistic habitable zone respectively.

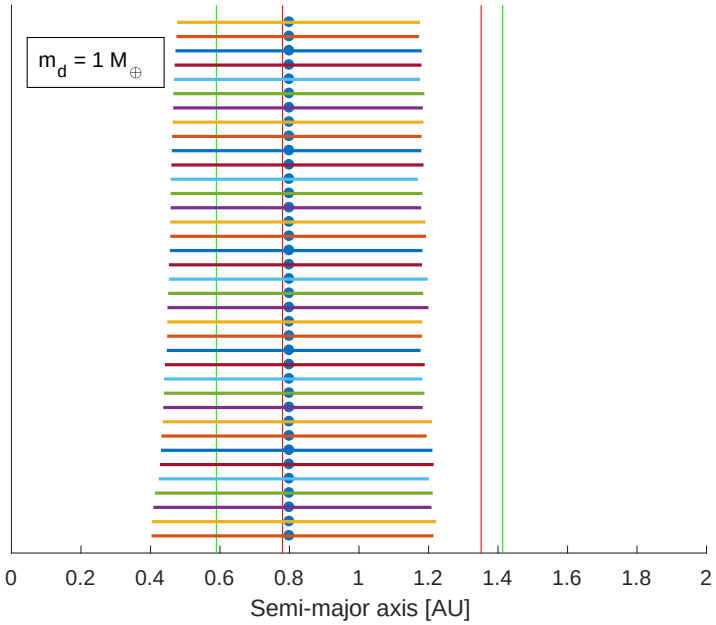

Figure A.0.1: 1 $M_\oplus$ planet at 0.8 AU.

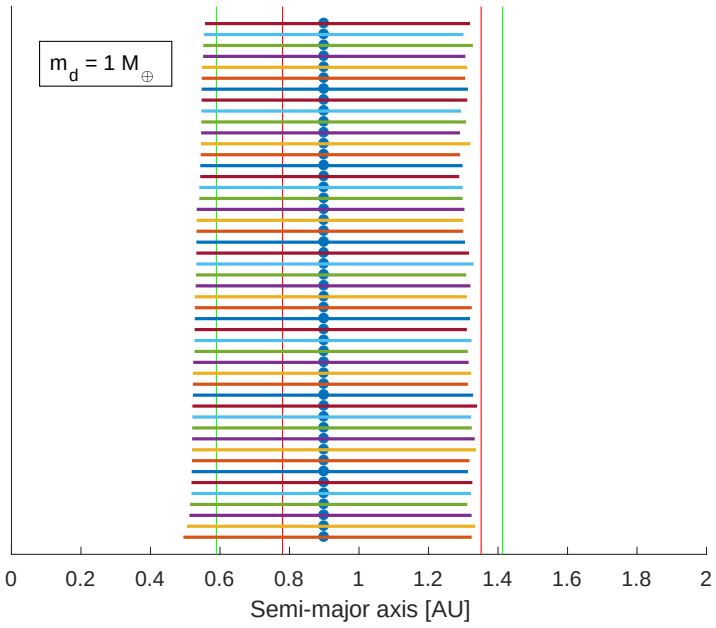

Figure A.0.2: 1 $M_\oplus$ planet at 0.9 AU.

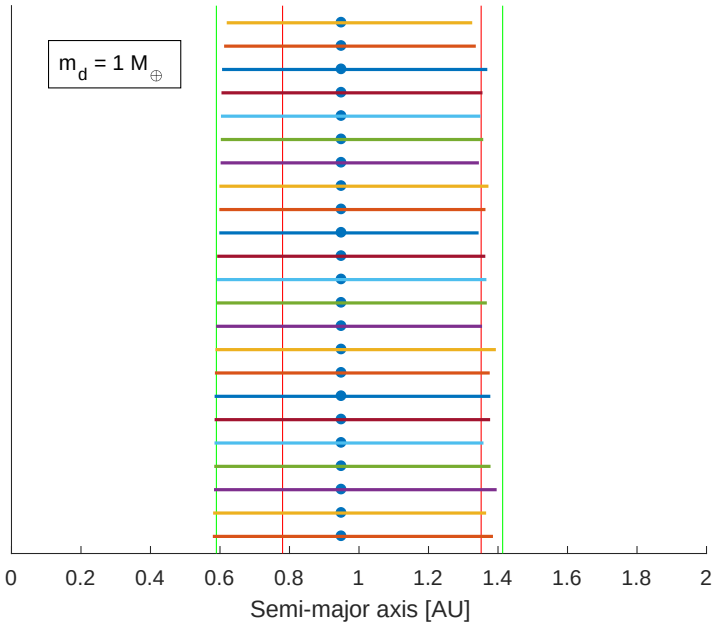

Figure A.0.3: 1 $M_\oplus$ planet at 0.95 AU.

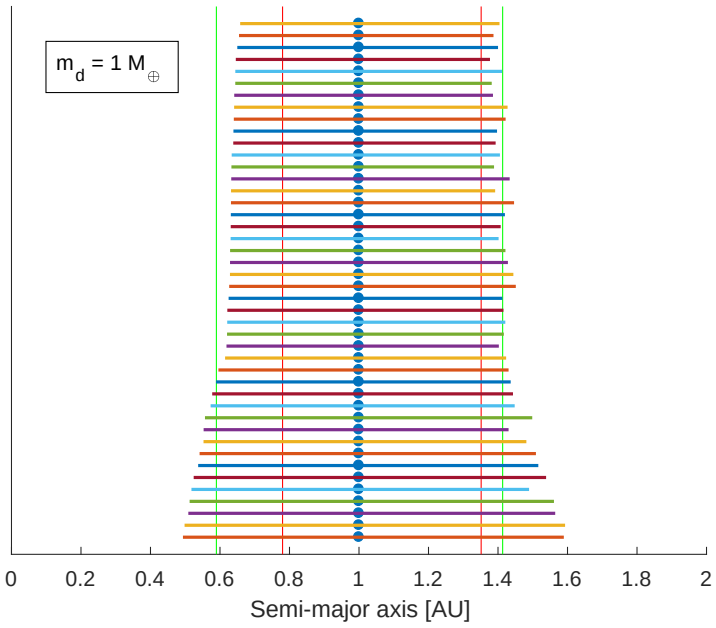

Figure A.0.4: 1 $M_\oplus$ planet at 1 AU.

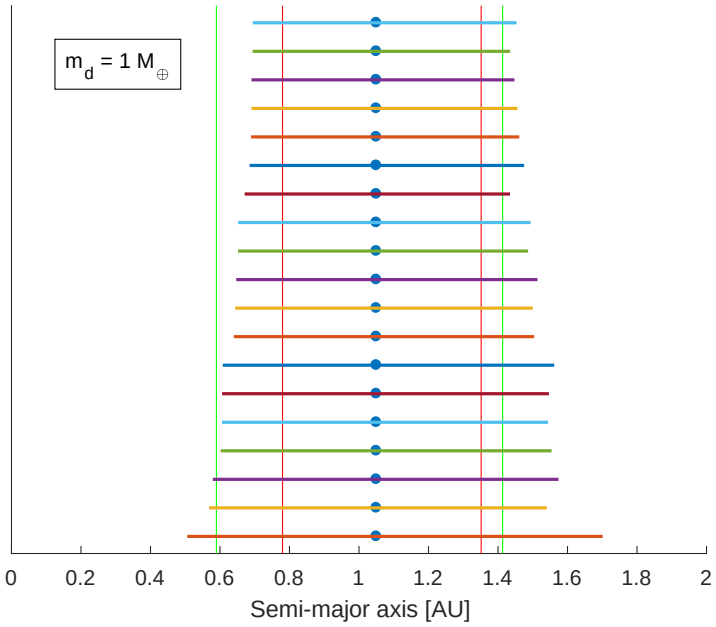

Figure A.0.5: 1 $M_\oplus$ planet at 1.05 AU.

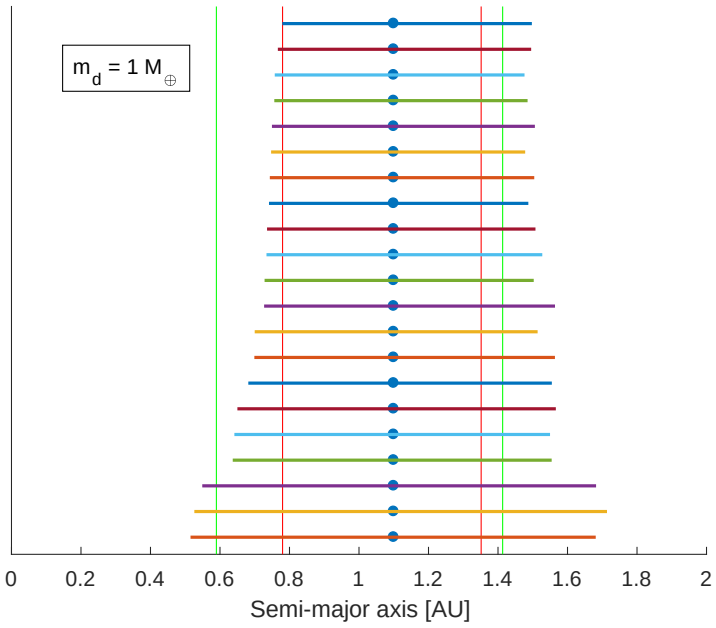

Figure A.0.6: 1 $M_\oplus$ planet at 1.1 AU.

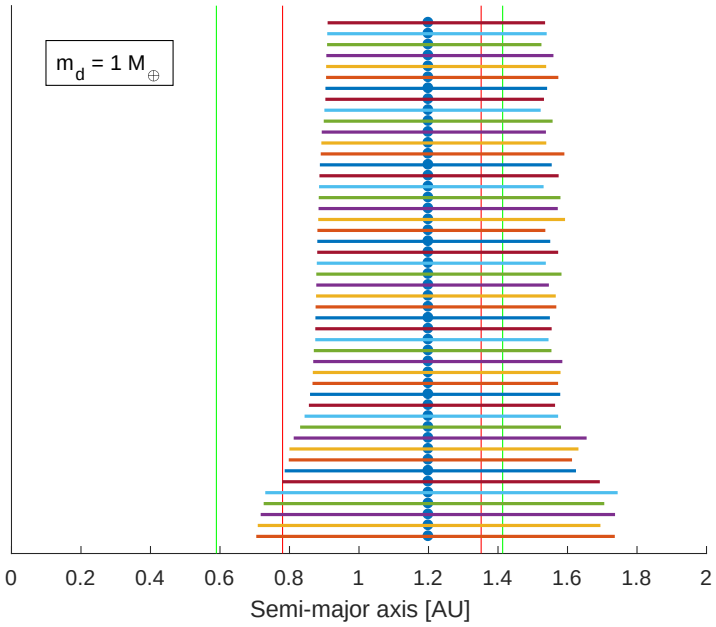

Figure A.0.7: 1 $M_\oplus$ planet at 1.2 AU.

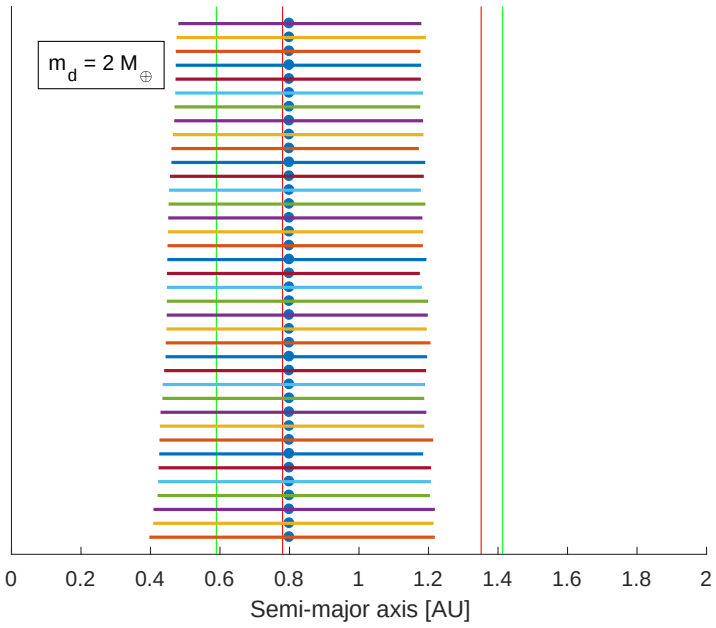

Figure A.0.8: 2 $M_\oplus$ planet at 0.8 AU.

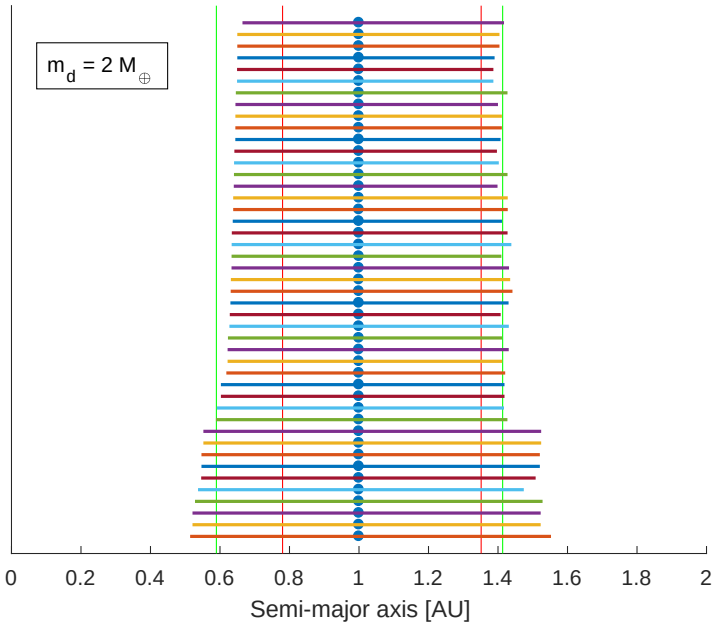

Figure A.0.9: 2 $M_\oplus$ planet at 1 AU.

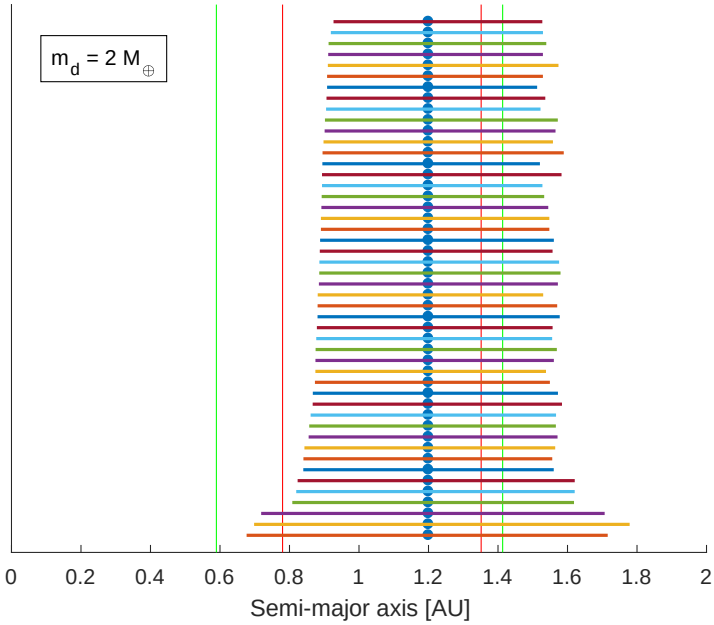

Figure A.0.10: 2 $M_\oplus$ planet at 1.2 AU.

Appendix B

Energy in an elliptical orbit

The total orbital energy of a planet is the sum of the kinetic and potential gravitational energy. In a two-body system, where there is only one planet and a star the energy is given by

$$E = \frac{1}{2}M_1 v^2 - \frac{GM_1M_2}{r}. \tag{B.1}$$

Where M_1 is the mass of the planet, M_2 the mass of the star, and r the distance to the star1. The velocity of a planet on an elliptical orbit is given by

$$v^2 = GM_2\left(\frac{2}{r} - \frac{1}{a}\right) \tag{B.2}$$

(Szebehely & Mark 1998). Where a is the semi-major axis. However, at some point in the orbit the distance to the star is equal to the semi-major axis. At this point, where $r = a$, the velocity simplifies to

$$v^2 = \frac{GM}{a}, \tag{B.3}$$

and inserting this into the total energy equation gives

$$E = \frac{GM_1M_2}{2a} - \frac{GM_1M_2}{a} = -\frac{GM_1M_2}{2a}. \tag{B.4}$$

Since the total energy must be conserved, if this is the total energy at some point in the orbit, it must be the total energy at any point in the orbit.